A Finite Element Analysis for Predicting the Residual Compression Strength of Impact-Damaged Sandwich Panels

James G. Ratcliffe
Senior Research Scientist
National Institute of Aerospace, Hampton, VA 23666
Resident at Durability, Damage Tolerance and Reliability Branch
NASA Langley Research Center, Hampton, VA 23681

Wade C. Jackson
Aerospace Engineer
Durability, Damage Tolerance and Reliability Branch
NASA Langley Research Center, Hampton, VA 23681

ABSTRACT: A simple analysis method has been developed for predicting the residual compression strength of impact-damaged sandwich panels. The method is tailored for honeycomb core-based sandwich specimens that exhibit an indentation growth failure mode under axial compression loading, which is driven largely by the crushing behavior of the core material. The analysis method is in the form of a finite element model, where the impact-damaged facesheet is represented using shell elements and the core material is represented using spring elements, aligned in the thickness direction of the core. The nonlinear crush response of the core material used in the analysis is based on data from flatwise compression tests. A comparison with a previous analysis method and some experimental data shows good agreement with results from this new approach.

1. Introduction

Rotorcraft designs typically include sandwich construction made from thin facesheets and lightweight cores. This type of structure is very susceptible to damage from out-of-plane loading such as low-velocity impact. These structures must be designed to sustain ultimate load with barely visible impact (BVID) damage. BVID can result in a strength reduction of 50% or more relative to an undamaged structure [1]. The failure mechanics of impact-damaged, thin-skin sandwich structure are not well understood, and analytical models are not currently used to predict the compression after impact (CAI) strength. Consequently, the design allowables for sandwich structure are normally obtained empirically using coupon and component testing. Analytical tools are needed to predict the performance of an impact-damaged sandwich structure that can be used during the design process to develop optimized structures.

Impact damage typically consists of a combination of facesheet damage (matrix cracking, delamination, and/or fiber breakage), core debonding, and core crushing. In addition, a residual dent is typically formed around the point of out-of-plane loading. In order to measure the residual compression strength of impact-damaged sandwich panels, the specimens are subjected to an axial compressive load using a test configuration similar to that shown in Figure 1. Two basic failure mechanisms [1] have been identified that lead to structural failure during these axial compressive tests: kink-band propagation and indentation growth. Figure 2 shows shadow moiré images of failure sequences from the two failure modes. With kink-band propagation (Figure 2a), the damage acts as a

stress concentration similar to an open hole. As a compressive load is applied, the tows or fibers in the loading direction buckle and break normal to the plane of the facesheet, creating a band of broken fibers that propagates perpendicular to the loading direction. This kink-band continues to slowly propagate away from the damaged region with increasing load until a critical length is reached where the kink band suddenly grows across the width causing failure. For the indentation-growth failure mode (Figure 2b), the residual indentation from the impact buckles inward and expands as the compressive load increases. The local buckle in the facesheet applies compressive loads to the core, causing additional crushing as well as elastic deflections. When a critical compressive force is reached, the facesheet rapidly buckles across the width and fails.

Analysis methods have been developed to predict the residual compression strength of specimens containing though-thickness slits or holes, where the specimens exhibit kink-band propagation failure [2-7].

A number of analyses have been developed for predicting the residual compression strength of sandwich specimens exhibiting the indentation growth failure mode [8-13]. An analytical model to understand and predict this type of failure was first developed by Minguet [8]. In this analysis, both facesheets were modeled using thin plate theory, and the core was modeled as a homogeneous solid. This model did lead to a greater understanding of the indentation growth failure mode. However, the model is complex and involves a number of limiting assumptions during analysis development. The facesheet is assumed to be unsupported by the region of core damaged during the impact. Consequently, the model does not capture the initiation of core crushing. Further, the loading condition used in the analysis is in the form of a constant force along the specimen width, whereas compression tests apply a constant displacement along the specimen width.

Other researchers [9-11] have made several modifications to Minguet's analysis since its development. A simplified version of the analysis was developed by Tsang [9], where a two-parameter, elastic core model was used, and only the impact-damaged facesheet was included in the analysis. Moody [10] reported that these two analyses failed to accurately predict the initiation of the indentation propagation. Some experimental work may suggest that facesheet damage will affect the compression strength and should be incorporated into the failure analysis [11].

As a result of this finding in Ref. 11, Tsang's analysis [9] was modified to include impact damage in the facesheet (modeled by a region of reduced stiffness centered around the impact location) [12]. It was found that this reduced stiffness model only had a small effect on specimen response. Xie [13] later modified this analysis to include angle ply facesheets, an equivalent one-parameter core model and an improved model for the initial propagation of the impact-damaged region. A "plateau" core strength instead of the undamaged core strength was used to achieve good correlation with some experimental results.

In summary, there has been a significant effort towards predicting the residual compression strength of sandwich specimens exhibiting indentation growth failure. However, in all of these cases, the analyses are either prohibitively complex, and/or the assumptions used result in some limitations or misrepresentations of the sandwich panel being modeled. Therefore, the objective of this paper was to develop an analysis tool that is practical to use in terms of technical complexity and computational efficiency, whilst

retaining a reasonable representation of the impact-damaged sandwich specimen. The remainder of this paper discusses specimen configurations considered, analyses developed, results of a series of parametric studies, comparison with previous analysis and a few concluding remarks.

2. Impact Damaged Sandwich Panels

A typical sandwich panel specimen used for compression testing consists of a low-density core reinforced by thin, laminated, composite facesheets. The core material is usually an aluminum or Nomex®[1] honeycomb construction, with a thickness in the range of 3.2mm to 50mm. Sections of the core material are replaced with a potting compound at the loading ends of the compression specimen. The potting serves to reinforce the facesheet during loading, which prevents damage.

Prior to compression testing, the specimens are struck with a drop weight impactor, creating damage in one facesheet. A picture of a typical sandwich specimen (post impact test) is given in Figure 3a. Specimen sectioning reveals that a significant region of core is crushed during the impact event. The area of this core crush region is typically greater than the dent area, which is visible from inspection of the facesheet. An example of the core crush due to the impact event is shown in Figure 3b.

The residual compression strength of these panels is then measured by subjecting the damaged panels to a uniaxial compression load (Figure 1). The residual strength is calculated by dividing the failure force measured in the test by the cross-sectional area of both facesheets.

3. Analysis Development

3.1 Sandwich Panel Model

In the current method, a finite element model is used to represent the impact-damaged sandwich panel. The commercial finite element analysis code, ABAQUS®[2]/Standard [14], was used to perform the finite element analysis. A FORTRAN routine was written to generate the finite element mesh automatically. The routine allows the user to vary parameters of the finite element model, such as panel size, facesheet stacking sequence, core thickness, mesh density and so forth. The damaged facesheet is represented using 4-node shell elements (ABAQUS® element type S4). Double axis symmetry (along the x-and y-axes) is assumed in order to reduce the model size. A typical finite element mesh is given in Figure 4. The damage imparted into the facesheet as a result of the impact event is represented in this analysis as a residual dent using the following expression for the nodal z-coordinate. A similar approach was used in the analysis described in Ref. 8.

$$z(x,y,R_d z_o) = \frac{z_o}{4}\left[1+\cos\left(\frac{x}{R_d}\right)\right]\left[1+\cos\left(\frac{y}{\sqrt{R_d^2-x^2}}\right)\right] \qquad y < \sqrt{R_d^2-x^2} \tag{1}$$

The coordinates are with respect to the system shown in Figure 4. The terms R_d and z_o refer to the indentation radius and maximum indentation depth, respectively.

---

[1] Nomex® is a registered trademark of E.I DuPont de Nemours, Wilmington, DE, USA

[2] ABAQUS® is manufactured by Dassault Systèmes Simulia Corp. (DSS), Providence, RI, USA

The undamaged (back surface) facesheet is not considered in this analysis, on the assumption that the force distribution between the undamaged and damaged facesheets is approxiamately equal. A previous study demonstrated this assertion to be valid for sandwich panels containing the level of impact damage of current interest [6].

The core material is modeled using 2-node spring elements (ABAQUS® element type SPRINGA). The elements are intended only to simulate the normal stresses acting on the facesheet as a result of deformation in the core material. The length of the undamaged springs was set equal to the thickness of the core material (in this case 25mm). The compressive response of the core material through the core thickness direction (*z*-axis in this analysis) is significantly affected by crushing from the impact event. This is accounted for in the analysis by assigning a circular region of spring elements that have a stiffness relationship corresponding to that of crushed core. This region is located concentrically about the center of the residual dent in the facesheet. The remaining spring elements are assigned a stiffness relationship that corresponds to that of undamaged core material. An illustration of this spring stiffness assignment is presented in Figure 4, where the shell element nodes that connect to the spring elements are color-coded. Red nodes indicate the position of spring elements used to represent core that was crushed by the impact event. Gray nodes indicate the location of spring elements representing the initially undamaged core. Further details of the material model used to represent the behavior of the core material are given in Section 3.2. The gold colored nodes shown in Figure 4 represent the location of the potting material in the sandwich specimen.

The modulus of the potting material used in the specimens (typically a syntactic foam) is significantly greater than the thickness-direction modulus of honeycomb core materials. Therefore, the potted region of the specimen was assumed to be rigid in the core thickness direction. This was simulated in the analysis by assigning boundary conditions to the potting region nodes, which prevent displacement in the core thickness direction (*z*-axis). Boundary conditions are assigned to satisfy the *x*-axis and *y*-axis symmetry conditions along the appropriate node locations, as indicated in Figure 4.

The uniaxial compression load applied to the specimens was modeled by prescribing a uniform displacement along a set of nodes, in the global *y*-direction, as indicated in Figure 4. Use of the prescribed displacements in the finite element analysis ensured that the load application was representative of the loading conditions used in compression tests. Each analysis was run in a number of increments, where the maximum increment size was limited to 1% of total applied displacement in order to accommodate for the nonlinear stiffness relationship of the spring elements. The maximum increment size used in the analyses was determined by repeating a preliminary analysis with different increment sizes. A value of 1% was chosen on the basis that analysis results were not sensitive to values in this range. For all the analyses performed, the nonlinear solution option in ABAQUS®/Standard was used.

3.2 Core Damage Model

In the current analysis, crushing of the core material is assumed to be the only damage mechanism involved in the indentation growth failure mode. This assumption was made on the basis of observations made of the indentation growth failure mode during previous experiments [1].

As noted in the previous section, the compressive response of the honeycomb core material (in the thickness direction of the core or *z*-axis in the current analysis) is significantly affected if it was previously crushed. Consequently, the finite element model contains two groups of spring elements. The first group represents core that was crushed from the impact event and the second group represents the undamaged core. The nonlinear compression response used to model crush behavior of the undamaged core material is based on the response measured from a flatwise compression test. During this test, a compressive force is applied normal to the facesheet of a square specimen (typically 1 to 4 inches square), as illustrated in the schematic in Figure 5. The compressive force-displacement behavior typically includes an initially linear response, proceeded by an unstable force drop, corresponding to buckling of the honeycomb cell walls. A typical crush response from an actual flatwise compression test on a Nomex® honeycomb-based sandwich specimen is given in Figure 6. The critical force associated with the force drop is termed F_{cc} (Figure 6). Upon further loading, core crushing continues, resulting either in a constant force (termed here as F_{crush}, Figure 6) or a gradual increase in force with further end shortening of the specimen. The idealized crush behavior (dotted blue line), as would be used in the current method, is superimposed onto the experimental plot in Figure 6. It was assumed that pre-crushed core material follows the compressive response depicted by the red dotted line in Figure 6 (note, the post crush portion of each law coincides and appears offset for illustrative purposes).

Preliminary parametric studies conducted using the current analysis indicate that the elastic, thickness-direction, tension modulus of the core material significantly affects the predicted compression behavior of the impact-damaged sandwich specimen. If this modulus value is too small, the analysis underestimates the global stiffness of the sandwich specimen in compression. The tensile and compressive moduli are expected to differ due to the out-of-plane deformation of the honeycomb wall cells that develop in compression but not in tension. Subsequently, a non-zero value of the core tension (thickness-direction) modulus is assumed in the analysis. In the absence of test data of this modulus value, a parametric study was performed to estimate an appropriate value for the core tension modulus. This study is described later in Section 4.5.

A summary of the assignment of the two core models in the current analysis procedure is given in Figure 7. Tensile stress is included in the schematics of the core models to indicate that a non-zero value of core tension modulus (in the core thickness direction) was used. In both core models, the tension response was assumed to be linear, as illustrated in Figure 7.

3.3 Mesh Density

This finite element analysis procedure was expected to exhibit some sensitivity to mesh size, since the core is represented at discrete locations using spring elements. Subsequently, a series of ten analyses were conducted, each consisting of a different number of degrees of freedom (dof). The residual strength computed from each analysis is plotted in Figure 8 as a function of the number of dofs in each model. This result highlights that the residual strength converges after the model size is increased above 28000 dofs, and it is therefore assumed that analyses with 28000 or more dofs yield a converged solution. On the basis of the results from this study, all other analyses were performed using models containing approximately 54000 dofs. The larger model was

used in order to ensure that the indentation region of the model was represented to a very high degree of accuracy.

3.4 Analysis Procedure

The analysis is conducted in several stages. In the first stage, the finite element mesh is generated using the FORTRAN routine described in Section 3.1. A prescribed displacement is applied to the model at the location indicated in Figure 4a. A geometrically nonlinear static analysis is performed in order to capture the nonlinear response of the specimen associated with large facesheet deformations and nonlinear core crushing. Each analysis is run with a maximum increment of 1% of the total prescribed displacement. At the end of each displacement increment, the far-field force applied to the specimen is calculated. This force is calculated by summing the reaction force (along the prescribed displacement direction) at each node to which a prescribed displacement is applied (see Figure 4a). The force values are then plotted as a function of prescribed displacement for each displacement increment, resulting in the computed force-displacement response of the specimen. An example of this computed force-displacement response is given in Figure 9. The initial force-displacement response is linear, but becomes slightly nonlinear as the maximum force is reached. After this point, further displacement results in a rapid decrease of force. The maximum force (indicated as Point 4 in Figure 9) is therefore assumed to correspond to failure of the sandwich panel. The corresponding residual compression strength is then computed as the maximum force divided by the net section area of the facesheet modeled (in this case, half the width of one facesheet, as only the damaged facesheet is considered in the current analysis). Contour plots are also included in Figure 9 and show the computed out-of-plane displacement of the facesheet at various stages of the force-displacement response (red and blue correspond to maximum and minimum values of out-of-plane displacement, respectively). The displacement contours exhibit the same behavior as observed experimentally, Figure 2b.

4 Parametric Studies

Three parametric studies were conducted as part of a preliminary evaluation of the current analysis method, which are described in this section.

The sandwich specimen analyzed during the parametric studies was the same as the specimen modeled by Minguet [8]. The analyses modeled a quarter section of a 80mm by 80mm sandwich panel consisting of a 25mm-thick Nomex honeycomb core (with a density of 48kg/m^3), reinforced with two facesheets, consisting of two plies of T800/F3900 plain-weave fabric, Figure 10. Each facesheet was assumed to be 0.5mm thick. The elastic properties of the sandwich panel used in the analyses are given in Table 1 [8]. The initial circular indentation (resulting from the assumed impact event) was 1mm deep and had a radius of 10mm (note that this indentation depth was varied in the study described in Section 4.1). The models relating to the crush behavior of the undamaged and crushed core regions are based on a core model used by Minguet [8]. Note that Minguet assumed the core crush radius to be 10mm [8]. In the current model, a 20mm radius core crush area is used based on observations, discussed in Section 2, that the core crush is often greater than the facesheet damage. A summary of the core models is given in Figure 11. Note that the elastic response of the core in tension (k_{ten}) is

included in the core models of undamaged and crushed core material. In both core models, the core tension stiffness was initially taken to be ten times the corresponding elastic compression stiffness (k_{comp}), as illustrated in Figure. 11. This was a preliminary value, and the effect of core tension stiffness on the analysis will be discussed in Section 4.3. It was assumed that a 10mm section of the core material was potted at the load application point, Figure 10. The potting extended across the entire specimen width.

4.1 Initial Indentation Depth

A series of analyses was conducted with different initial indentation depths ranging from one-fifth of a facesheet thickness to three facesheet thicknesses. The residual compression strength computed from each analysis is plotted as a function of initial indentation depth in Figure 12. In this figure, results from three of the analyses are highlighted (solid green disk indicates an initial dent depth equal to 0.4 times a facesheet thickness, solid black disk indicates an initial dent depth equal to one facesheet thickness, and solid red square indicates an initial dent depth equal to 1.4 times a facesheet thickness). The residual strength decreases by 10% as the initial indentation depth is increased from one-fifth of a facesheet thickness to three facesheet thicknesses.

This change in the residual strength is a result of a change in the stress distribution in the core for models with different initial dent depths. The distribution of though-thickness stress in the core material (σ_z) along the specimen mid-plane is given in Figure 13 for initial dent depths of 0.4, 1.0 and 1.4 times the facesheet thickness. The stress values are calculated using the axial force computed in the spring elements along the path of the calculated stress distributions. The three stress distributions correspond to the same applied in-plane compressive load (N_y) in the facesheet of 100 N/mm. For a given load, as the dent depth increases, the compressive stress (outside of the initially dented region) transmitted though the core material increases, Figure 13. Consequently, the applied, in-plane, compression load required for panel failure (corresponding to core crushing) decreases when the dent depth is increased to 3 times the facesheet thickness.

In summary, large increases in dent depth will lead to relatively small decreases in the computed residual strength. In the case of this study, an increase in dent depth of fifteen times the smallest value studied only resulted in a 10% decrease in the residual strength. Similar findings have been made experimentally by Cvitkovich and Jackson [1] and through analysis by Minguet [8].

4.2 Area of Initially Crushed Core

As discussed in Section 2, the area of core crushing, as a result of a low velocity impact event, typically extends beyond the visible dent in the impacted facesheet. The extent of this disparity, however, between dent diameter and core crush area is not well understood. Therefore, a study was conducted to determine the effect of core crush area on the computed residual compression strength. Nine analyses were conducted over a range of core crush areas including no core crushed and total core crushed. The diameter of the crushed area was increased up to the fully crushed case. In this case, the total core area was taken as the 40mm by 40mm section minus the 10mm by 40mm potted region (see Figure 10). Thus, in these examples, the total core area (A) was 1200mm^2. The force displacement responses computed from each analysis are presented in Figure 14. As expected, the residual strength reduces as the core crush area is increased. In this

figure, the core crush area is given as a fraction of the total core area, *A*. The reduction in residual strength is significant (difference in strengths between no core crushing and all core crushed models was 20%). Hence, the study suggests that an accurate measurement of the initial core crush area is important for improving the accuracy of the analysis.

4.3 Thickness-Direction Tension Stiffness of the Core

Results from preliminary analyses indicate that a significant amount of tensile stress is developed in the core material (along the core thickness direction) at the locations indicated in the insert of Figure 15. The stress distribution in the core material (in the core thickness direction) along Lines XX and YY are plotted in Figure 15. The results are from an analysis of the sandwich specimen described at the beginning of Section 4 and correspond to the peak applied force. A summary of the specimen details and core models are given in Figures 10 and 11, respectively. The stress distributions along Line YY show that a significant tensile stress is developed in the core, at the boundaries of the indentation. On the basis of this result, the tensile stiffness of the core (see Figure 11) is expected to significantly affect the predicted global response of the sandwich specimen. Furthermore, the tensile stiffness of the crushed core material will be very small compared to the compressive stiffness, due to the post-buckled state of the honeycomb cell walls. The observed dominance of compressive stress along Line XX may suggest why core crushing tends to advance along this direction.

In light that there is very little information in the literature regarding the through-thickness tension response of honeycomb materials (either crushed or undamaged), a series of studies was conducted to evaluate the sensitivity of computed specimen response to core tension stiffness. The model described above was used to conduct two studies. In the first study, the effect of the tension stiffness of the crushed and undamaged regions of the core on the computed specimen response was investigated. In the second study, only the tension stiffness of the crushed core was varied. In this case, the tension stiffness of the undamaged region was held constant at ten times the compression stiffness value. Both studies included several analyses each with a different value of core tension stiffness ranging from one tenth to ten times the corresponding compression stiffness value. The force-displacement response from each analysis was computed. The computed residual strength is plotted as a function of normalized core tension stiffness in Figure 16. The results show that the residual strength is highly sensitive to changes in core tensile stiffness, when the stiffness of both core regions was changed. The result also shows that residual strength converges after the core tensile stiffness is increased above five times the compressive stiffness value. However, the residual strength was moderately insensitive to changes in the tensile stiffness of only the crushed core region. In this case, changing the tensile stiffness of the undamaged core from one tenth of the compressive stiffness to ten times the compressive stiffness, only resulted in a 3% change in the computed residual strength.

As the residual strength is seen to converge at larger values of core tensile stiffness, in the current analysis method, the tension stiffness of the core will be assumed to be ten times the compression stiffness. This assumption will be made until future experimental measurements of core tension stiffness are made.

5 Comparison with Previous Analysis

In a previous analysis, Minguet [8] modeled the sandwich specimen described in Section 4 and summarized in Figures 10 and 11. In Minguet's analysis, the facesheets were modeled using Kirchhoff thin plate theory, and the core was modeled as a homogeneous solid. The displacements of the core and facesheet are represented by a series of harmonic functions. A nonlinear plate model is used to include the effect of the applied compressive loading on the transverse displacements of the dented facesheet. A core damage model uses a uniform grid over the facesheet to track the crush state of the core and apply discrete interface stresses accordingly. Some assumptions were made in the development of the model, including the assumption that no stress is transmitted through the region of crushed core. In the current analysis, the crushed core region is permitted to transfer stress through the thickness direction of the core. Additional assumptions include facesheet ends loaded using a uniform force and simply-supported boundary conditions. These assumptions are not required with the current analysis.

The elastic properties used in the analysis are given in Table 1. Due to the lack of data regarding the values of the maximum crushed core stress, F_{crush}, Minguet repeated the analysis three times using different values of the ratio, F_{crush}/F_{cc} (F_{cc} was known and kept constant at 1.8N/mm^2). Minguet computed specific displacement and stress distributions along the dotted lines shown in Figure 10 using $F_{crush}/F_{cc} = 0.6$. The current analysis was used to model this case, and comparisons with Minguet's analysis are made for the same displacement and stress distributions presented in Ref. 8. The force-displacement response of the panel, as computed using the current analysis, was also used to calculate the failure stress of the panel using the three ratios of F_{crush}/F_{cc} modeled previously by Minguet. These values are compared against Minguet's results and an experimentally-measured residual strength value reported in Ref 8.

5.1 Distribution of Transverse (z-axis) Displacements

The facesheet coordinates, w in the transverse direction, (including the initial dent depth) from Minguet's analysis and the current analysis are compared along Line XX for increasing values of force (N_y) in Figure 17. The results from both the analyses showed that the dented region in the facesheet expands perpendicular to the loading direction (Line XX) as the force applied to the panel increases. The transverse displacements along Line YY (loading direction) did not change significantly with loading and are not presented. These observations suggest that the initial facesheet indentation becomes elliptical as the sandwich panel is loaded. This behavior matches previously observed experimental responses [6, 8]. There are significant differences between predictions from the current analysis and Minguet's analysis, especially at larger applied forces. The predictions of the dent width agree well, but there are large differences in the displacements in the dented region. This difference is expected since Minguet's analysis assumes that the core material in the region of the initial dent does not transmit transverse stresses, whereas the initial dent region of the core in the current analysis is permitted to transfer stress.

5.2 Distribution of Transverse (thickness direction) Core Stresses

The transverse core stresses, σ_z, generated along Lines YY and XX are presented in Figure 18 for increasing values of force. Results from the current analysis indicate that

the transverse stress in the core is less than F_{cc} (see Figure 11) along Line YY, whilst the stresses reach F_{cc} along Line XX. Therefore, an elliptical dent shape will develop since the indentation will propagate along the *x*-direction but will remain fixed along the y-direction. Again, the results from both analyses differ, owing to the different stress distributions assumed in the initial dent region of the core. An additional result from the current analysis is included in Figure 18f. Here, the transverse stress distribution along Line XX is plotted at the force corresponding to panel failure. At this instance, the transverse stresses in the initially dented region of the core are equal to F_{crush}, and the stresses at the boundary of the dented region are at F_{cc}. It is also noted that the distance separating the peaks of compressive stress at failure load is larger than the initial core crush diameter. This indicates that an amount of core crushing takes place prior to complete panel failure.

5.3 Distribution of In-Plane Forces in the Facesheet

The distribution of the in-plane (*y*-direction) forces, N_{yy}, in the facesheet along Line XX are plotted in Figure 19, for increasing values of force. Results from Minguet [8] are included in the plots for comparison and show good agreement with results from the current analysis. The results indicate that the reaction forces in the facesheet in the direction of the applied force are not particularly sensitive to the assumed transverse stress distribution in the initially dented region of the core (this being the main difference between the two analyses). Since the predicted widths of the dent are nearly identical for the two analyses, the in-plane force N_{yy} are nearly identical. The slight differences between the two analyses are attributed to the different transverse displacements in the dented region.

5.4 Effect of Core Crush Behavior on Computed Failure Stress

As mentioned previously, the analysis was repeated for three different ratios of F_{crush}/F_{cc}, where F_{cc} remains fixed. The force-displacement responses calculated from the current analysis for the three core crush ratios are presented in Figure 20a. Failure of the sandwich panel occurs at the peak force, which corresponds to a rapid expansion of the width of the dent with corresponding core crushing. The resulting residual compression strengths of the sandwich panel with the three different core crush ratios are plotted in Figure 20b in addition to an experimental residual strength value ($250N/mm^2$ [8]). The same values were also calculated by Minguet [8] and are included in the plot for comparison. The comparison shows good agreement between the two analytical methods, illustrating that the assumed stress distribution in the initially dented core region does not significantly affect the computed failure stress for this case. Furthermore, according to the results from the current analysis, a 50% increase in F_{crush} only resulted in a 12% increase in the predicted failure stress. The residual strength computed using the current analysis was in better agreement (to within 5%) with the experimental value when the ratio F_{crush}/F_{cc} equaled 0.4. However, any significance of this comparison is limited owing to the limited amount of experimental data available for the sandwich panel considered.

6 Summary

An analysis method has been developed for predicting the residual compression strength of impact-damaged sandwich panels. The method is tailored for honeycomb core-based sandwich specimens that exhibit an indentation growth failure mode, which is driven largely by the crushing behavior of the core material. The analysis method is in the form of a finite element model, where the impact-damaged facesheet is represented using shell elements and the core material is represented using spring elements, aligned in the thickness direction of the core. The nonlinear crush response of the core material included in the analysis is based on flatwise compression tests conducted on samples of sandwich panel. The intact facesheet is not considered in the current analysis on the assumption that during a compression test, load is split equally between the two facesheets. A series of parametric studies were performed to identify parameters that were potentially important in the analysis. These studies indicated that the predicted compression response of the sandwich specimen is most sensitive to the initial core crush area (as a result of the assumed impact event) and the tension stiffness of the core material. Indeed further testing will be required to verify the current assumption that the tension stiffness of the undamaged core material should be approximately ten times the compression stiffness. The studies were also used to optimize the analysis procedure and ensure that the finite element analysis was yielding a converged solution.

A comparison of results from the current analysis against those of a previous, more complex method showed some differences in computed core stress and facesheet displacement distributions. These differences were explained by the difference in assumptions regarding stress distribution in the initially crushed region of core material. More importantly, the noted differences were not reflected in the comparison of the predicted failure stresses, which agreed to within 7% between the two methods. The current analysis also agreed well with an experimental value, although the reliability of this comparison is limited due to the small amount of experimental data available.

In general, the current analysis method appears able to capture the important aspects of the sandwich panel compression behavior, whilst remaining a relatively simple procedure to use.

Acknowledgements

This research was conducted at the Durability, Damage Tolerance and Reliability Branch, NASA Langley Research Center, VA and funded by the NASA Fundamental Aeronautics Program/Subsonic Rotary Wing Program

References

[1] Cvitkovich, M.K., and Jackson, W.C., "Compressive Failure Mechanisms in Composite Sandwich Structures," Journal of the American Helicopter Society, Vol.44 (4), pp.260-268, 1999.

[2] Toribio, M.G., Marizo, J.M., and Spearing, S.M., "Compressive Failure of Notched Composite-Honeycomb Sandwich Panels," Proc. 12th International Conference on Composite Materials, Paris, 1999.

[3] Marizo, J.M., and Spearing, M.S., "Damage Modeling of Notched Graphite/Epoxy Sandwich Panels in Compression," Applied Composite Materials, Vol.8(3), pp.191-216, 2001.

[4] Toribio, M.G., and Spearing, S.M., "Compressive Response of Notched Glass-Fiber Epoxy/Honeycomb sandwich Panels," Composites: Part A, Vol.32, pp.859-870, 2001.

[5] Kassapoglou, C., "Compression Strength of Composite Sandwich Structures After Barely Visible Impact Damage," ASTM Journal of Composites Technology and Research, Vol.18(4), pp.274-284, 1996.
[6] Ratcliffe J., Jackson, W.C., and Schaff, J., "Compression Strength Prediction of Impact-Damaged Composite Sandwich Panels," Proceedings of the American Helicopter Society 60th Annual Forum, Baltimore, MD, June 7-10, 2004.
[7] Soutis, C., and Fleck, N.A., "Static Compression Failure of Carbon Fibre T800/924C Composite Plate with a Single Hole," Journal of Composite Materials, Vol.24, pp.536-558, 1990.
[8] Minguet, P.J., "A Model for Predicting the Behavior of Impact-Damaged Minimum Gage Sandwich Panels Under Compression," AIAA/ASME/ASCE/AHS/ASC 32nd Structures, Structural Dynamics, and Materials Conference, Paper AIAA-91-1075-CP, 1991.
[9] Tsang, P. H. W., " Impact Resistance and Damage Tolerance of Composite Sandwich Panels," Ph.D. dissertation, Massachusetts Institute of Technology, June 1994.
[10] Moody, R. C., and Vizzini, A. J., "Incorporation of a Compliance Change Due to Impact in the Prediction of Damge Growth in Sandwich Panels," Proceedings of the 13th International Conference on Composite Materials, Beijing, China, June 2001.
[11] Tsang, P. H. W., and Lagace, P., "Failure Mechanisms of Impact-Damaged Sandwich Panels Under Uniaxial Compression," AIAA/ASME/ASCE/AHS/ASC 35th Structures, Structural Dynamics, and Materials Conference, Paper AIAA-94-1396-CP, 1994.
[12] Moody, R. C., and Vizzini, A. J., "Test and Analysis of Composite Sandwich Panels with Impact Damage," DOT/FAA/AR-01/124, U.S. Department of Transportation, Federal Aviation Administration, March 2002.
[13] Xie, Z., and Vizzini, A. J., "Damage Propagation in a Composite Sandwich Panel Subjected to Increasing Uniaxial Compression after Low-velocity Impact," Journal of Sandwich Structures and Materials, Vol. 7, No.4, pp 269- 288, 2005.
[14] ABAQUS®/Standard Version 6.7-2 User's manual, 2007.

Table 1. Facesheet Stiffness Properties [8]

Facesheet material: 2 plies T800/F3900 plain weave fabric Stacking sequence: [(0/90)/(0/90)]									
Thickness mm	E_x MPa	E_y MPa	E_z MPa	G_{xy} MPa	G_{yz} MPa	G_{xz} MPa	ν_{xy}	ν_{yz}	ν_{xz}
0.5	82351	82351	16508	6900	6376	6376	0.024	0.35	0.35

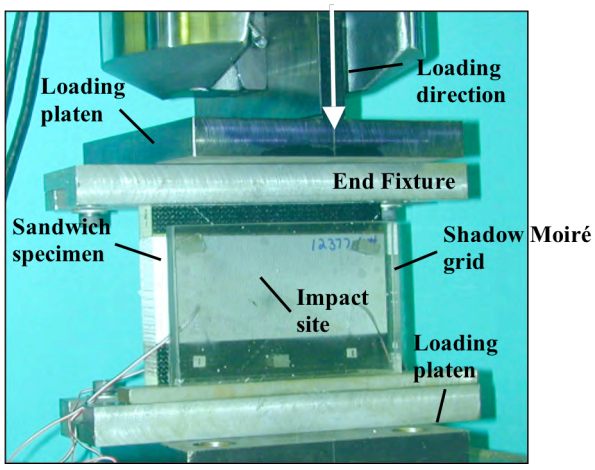

Figure 1. Test configuration of axial compression test on a sandwich specimen

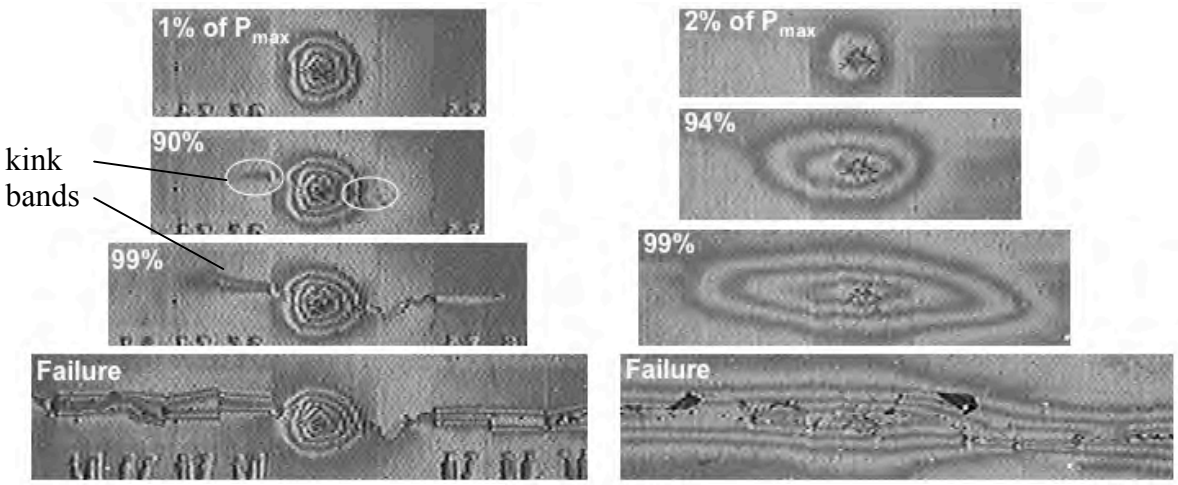

a. Kink-band propagation b. Indentation growth

Figure 2. Examples of compressive failure modes

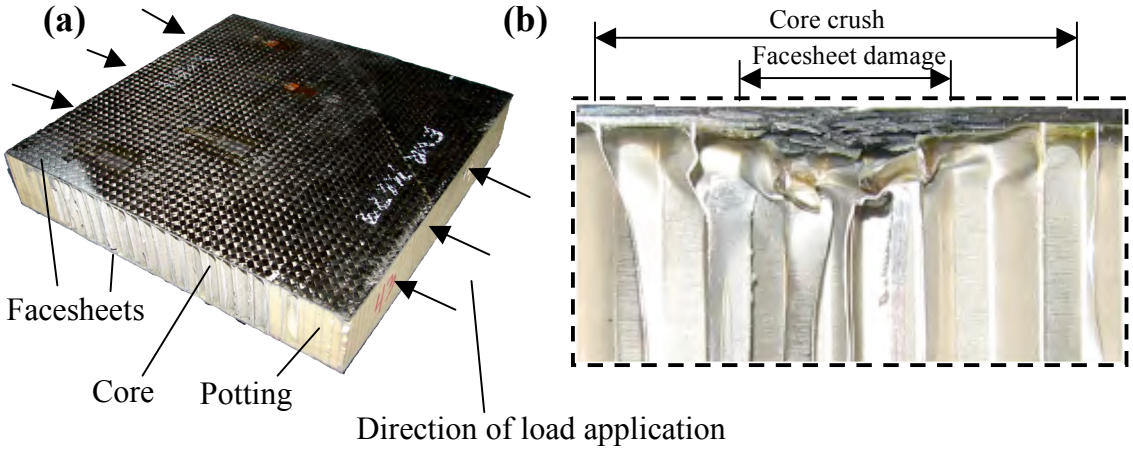

Figure 3. Impact-damaged sandwich panel and core crush resulting from impact

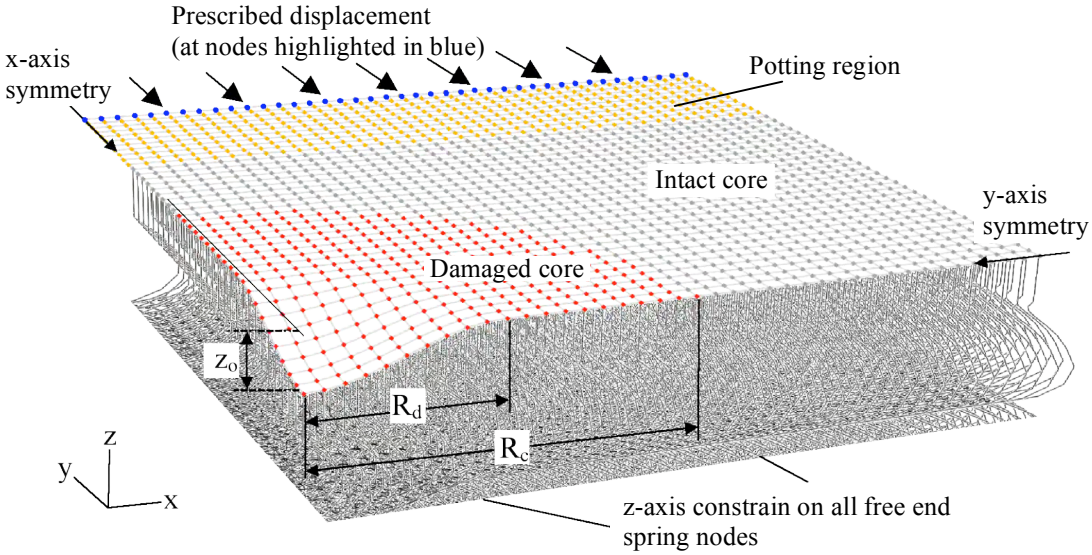

Figure 4. Finite element mesh used to model sandwich panel

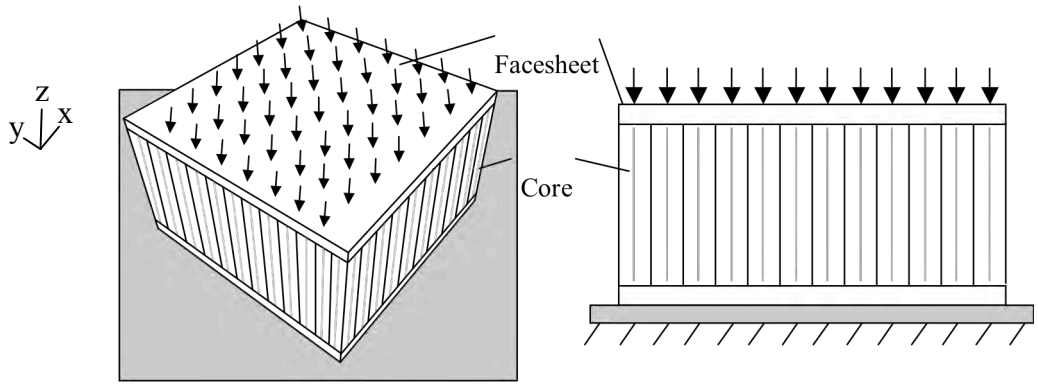

Figure 5. Flatwise compression specimen for characterizing core crush behavior

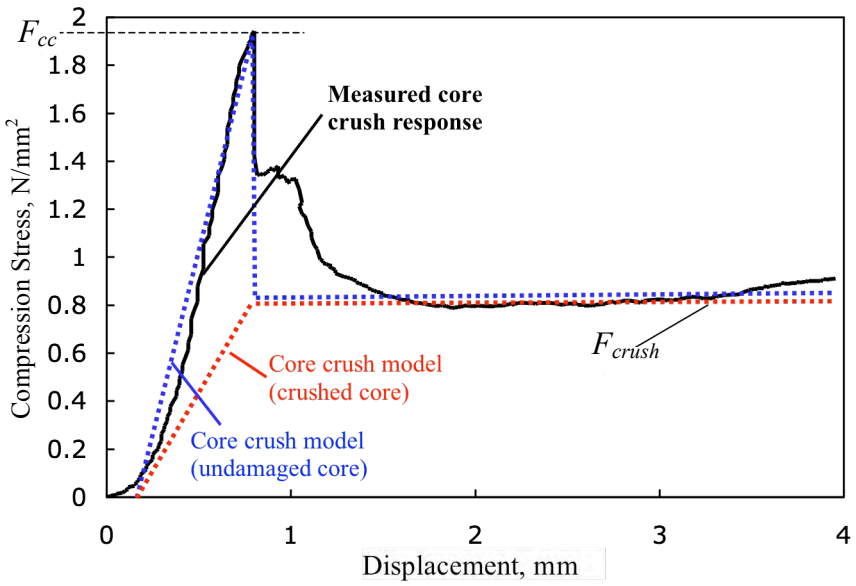

Figure 6. Measured and idealized core crush behavior

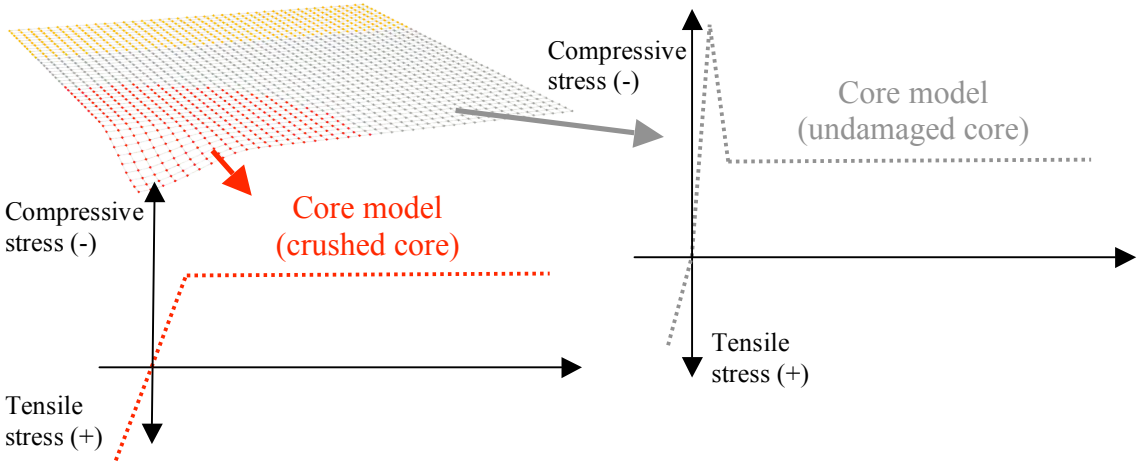

Figure 7. Summary of assignment of core models

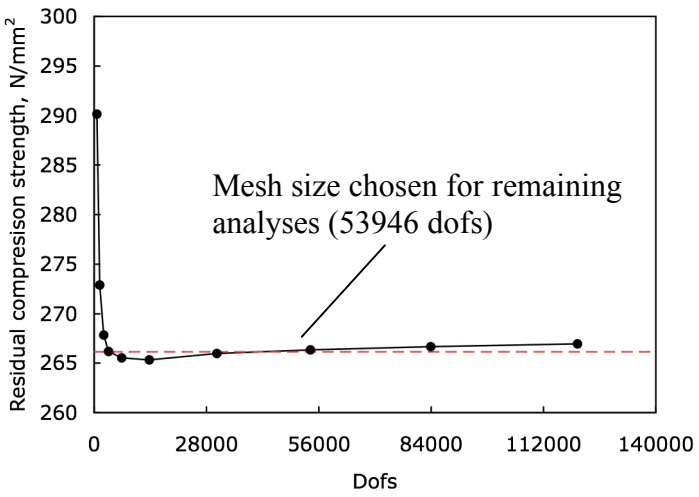

Figure 8. Effect of mesh density on computed residual strength

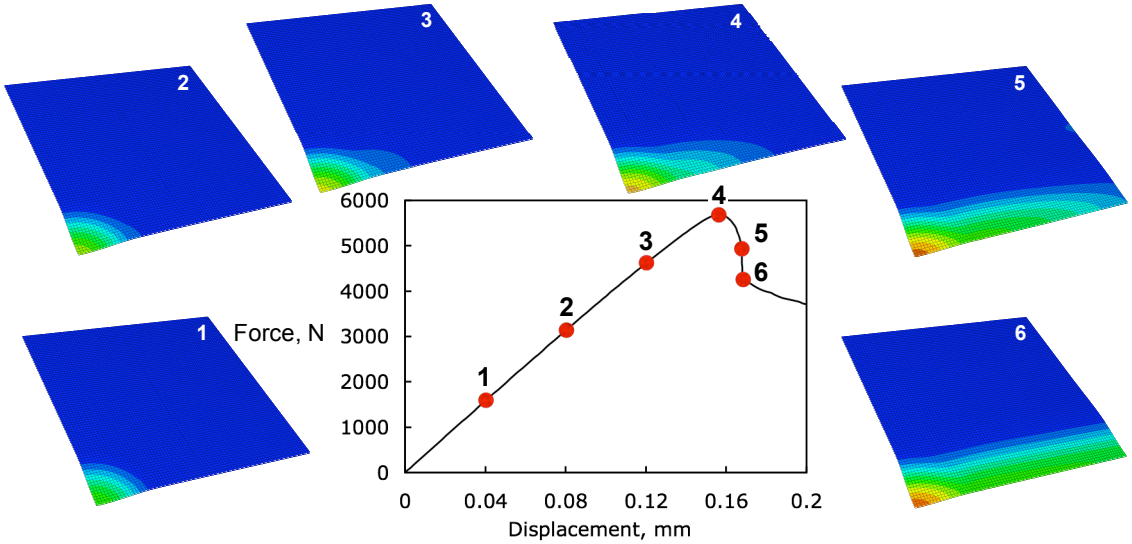

Figure 9. Typical computed force displacement response of sandwich specimen

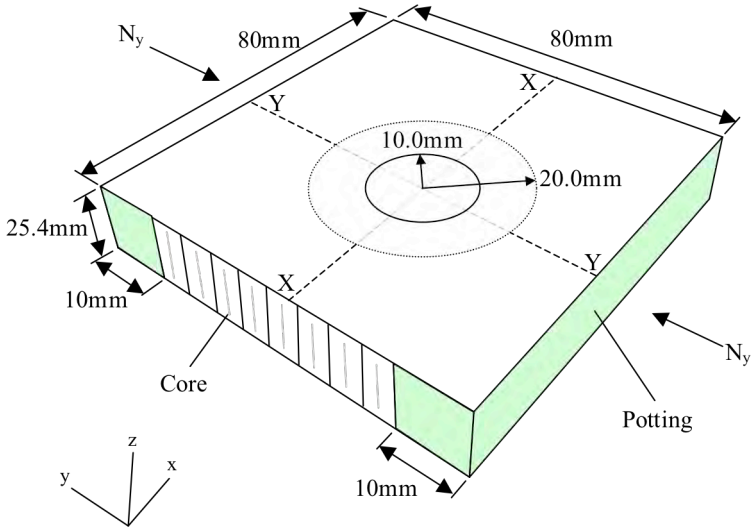

Figure 10. Schematic of sandwich specimen modeled in parametric studies

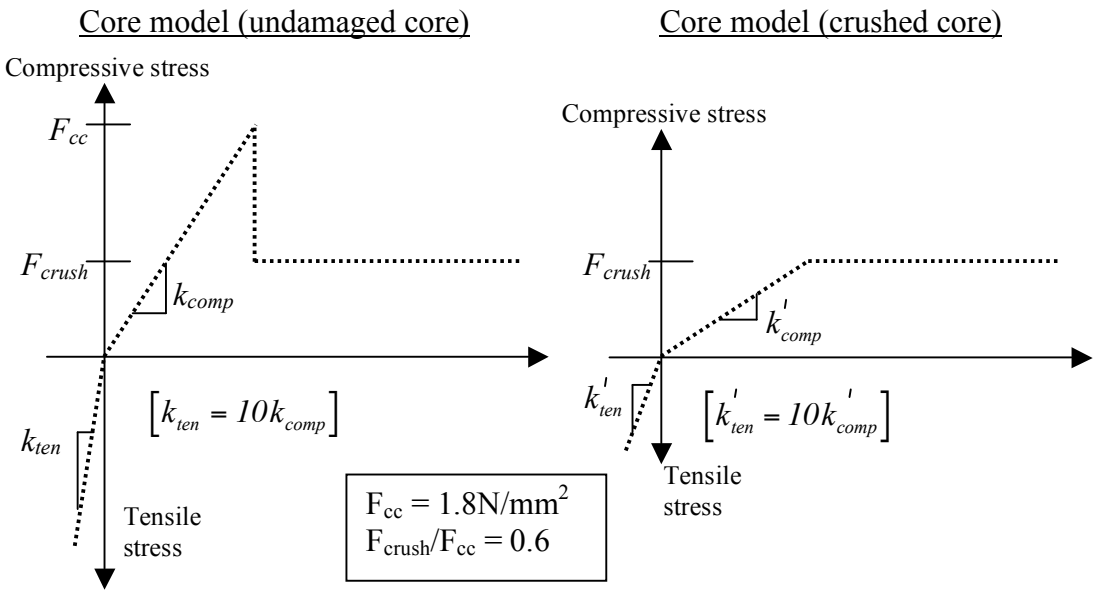

Figure 11. Core models used in parametric studies

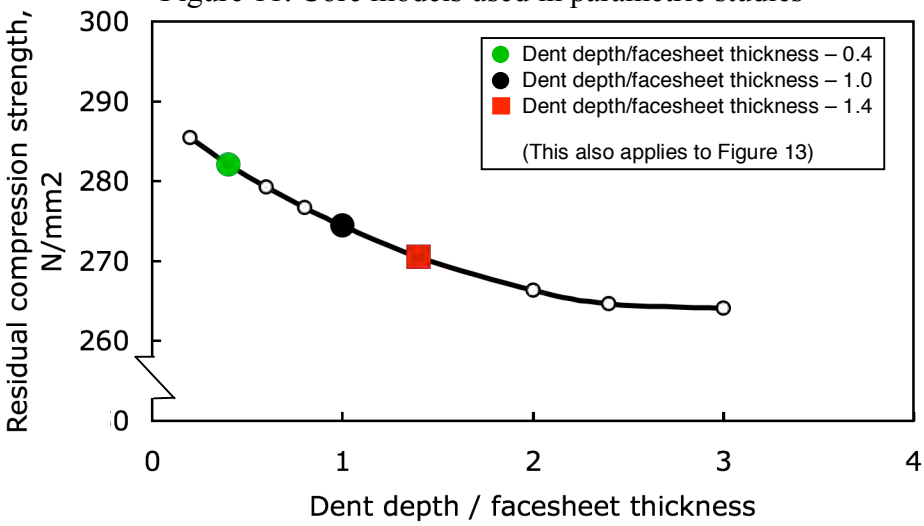

Figure 12. Effect of dent depth on computed residual strength

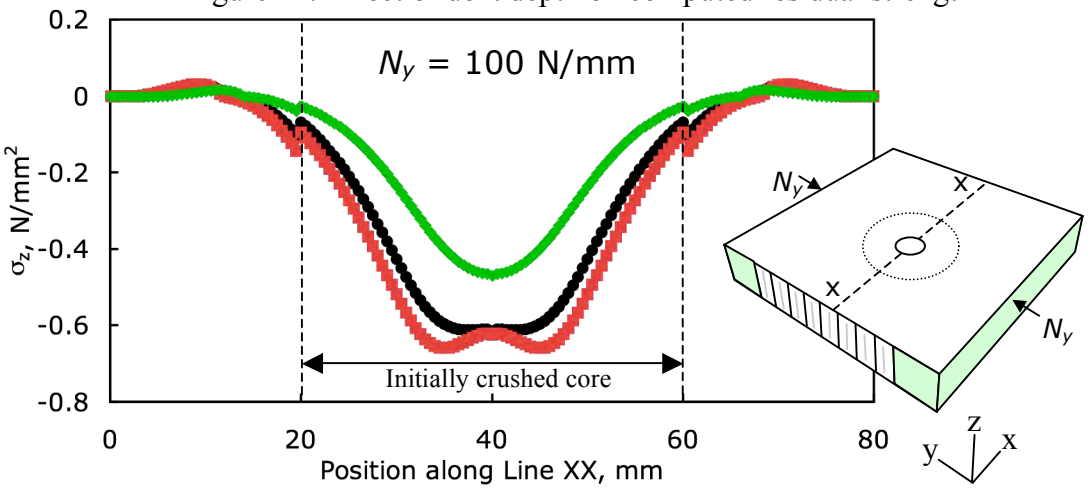

Figure 13. Thickness-direction stress distribution in core for analyses with different dents

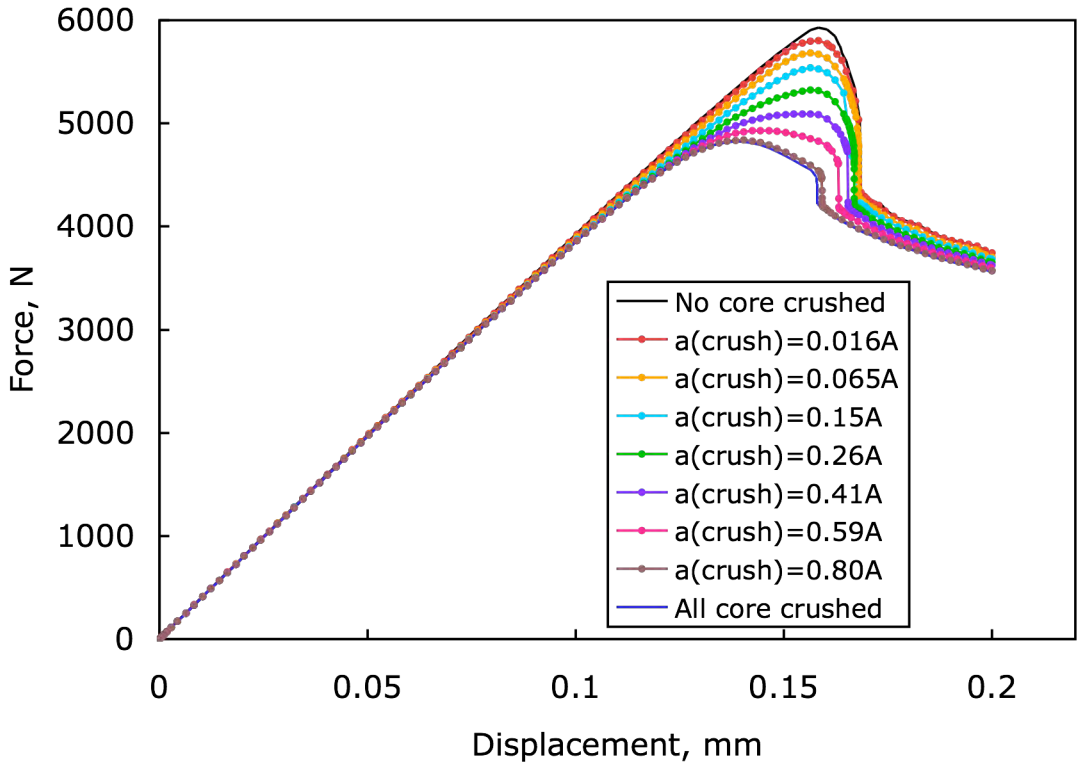

Figure 14. Force-displacement response from analyses with different core crush regions

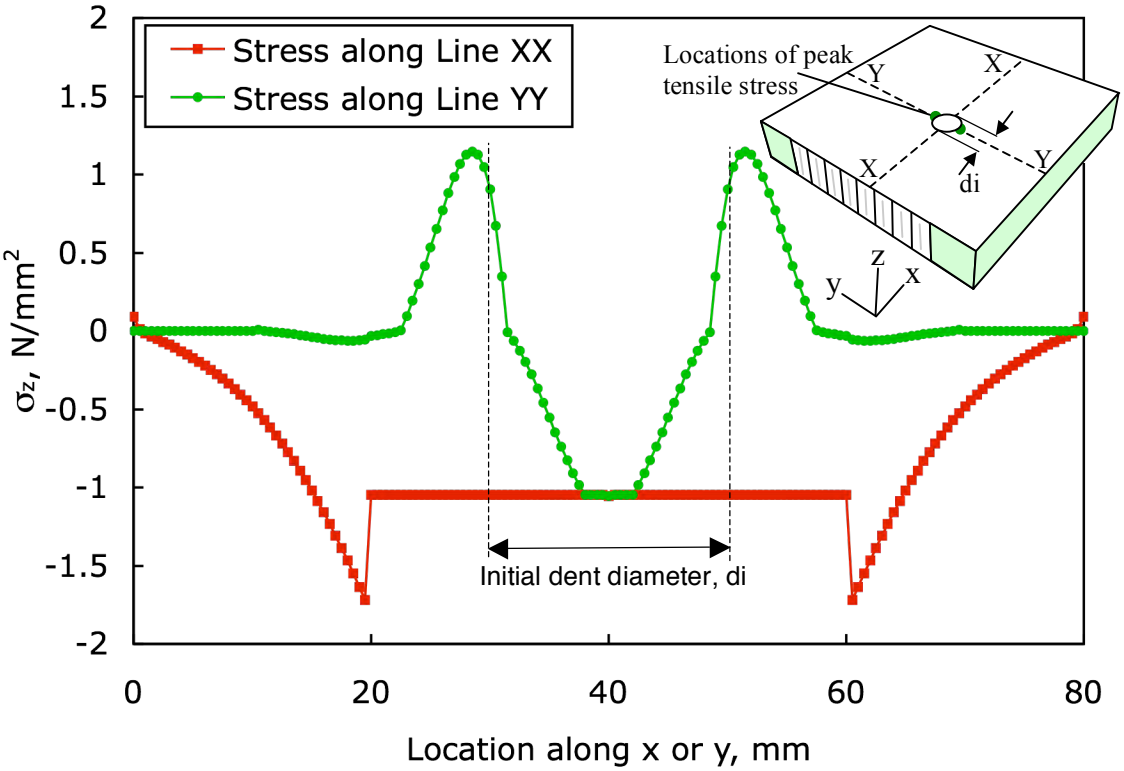

Figure 15. Thickness-direction core stresses along Lines XX and YY

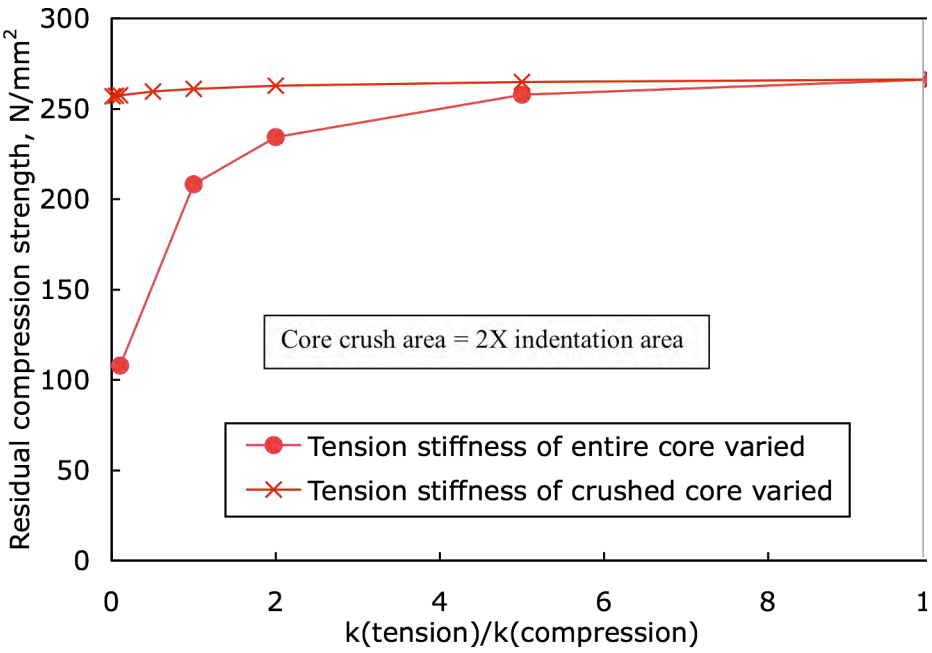

Figure 16. Effect of core tension stiffness on computed residual strength

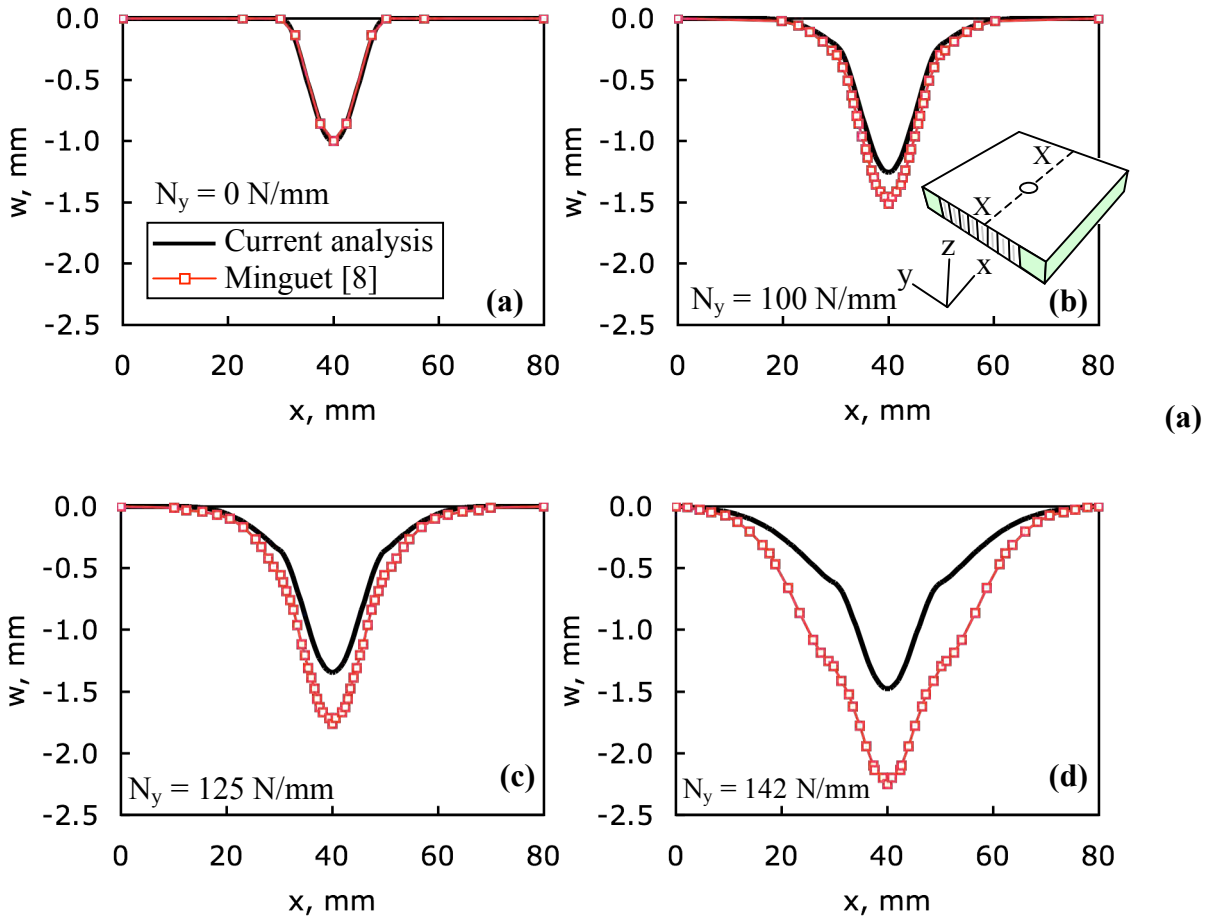

Figure 17. Transverse displacement along Line XX at various values of N_y

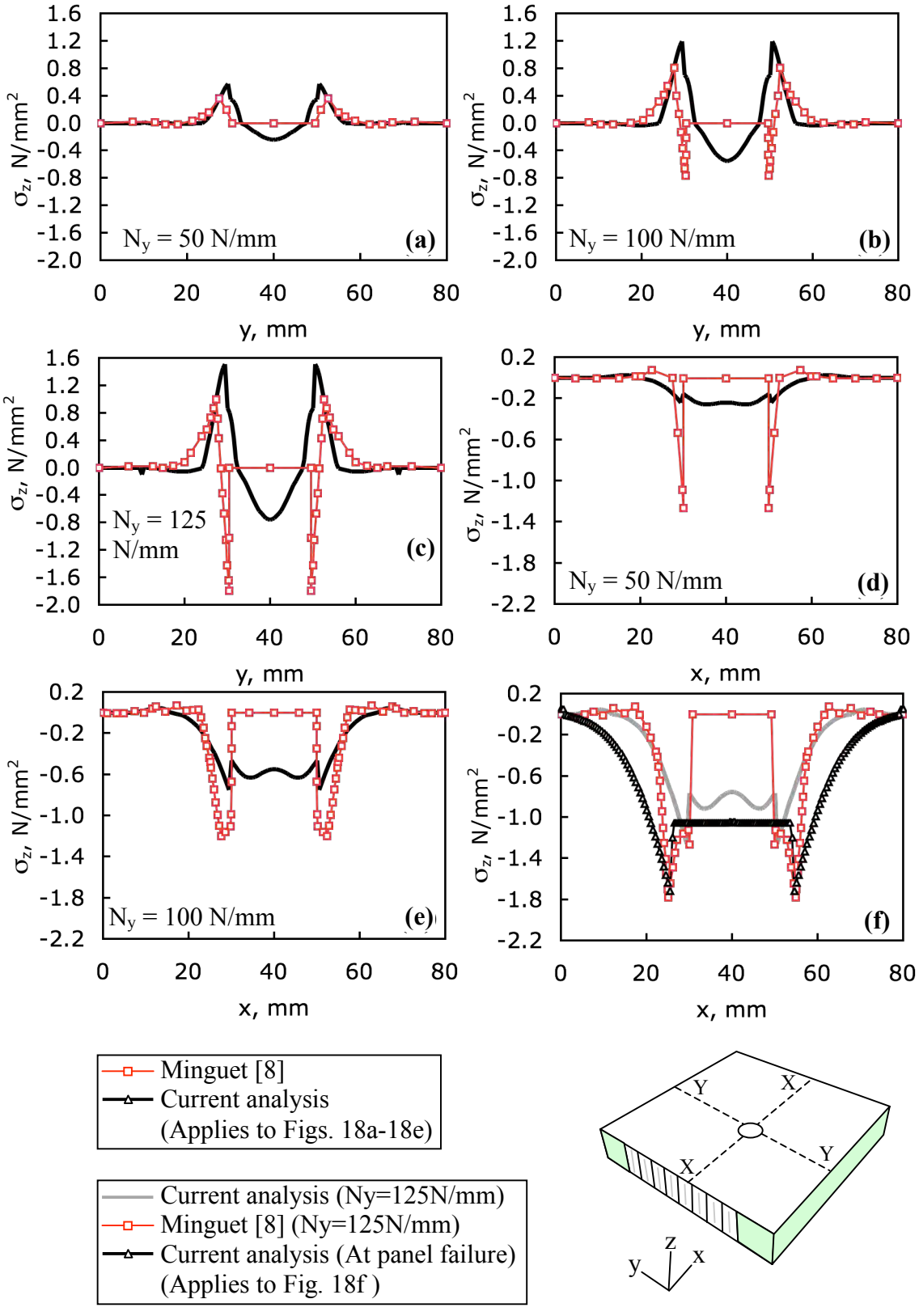

Figure 18. Z-axis core stresses along Lines XX and YY at various values of N_y

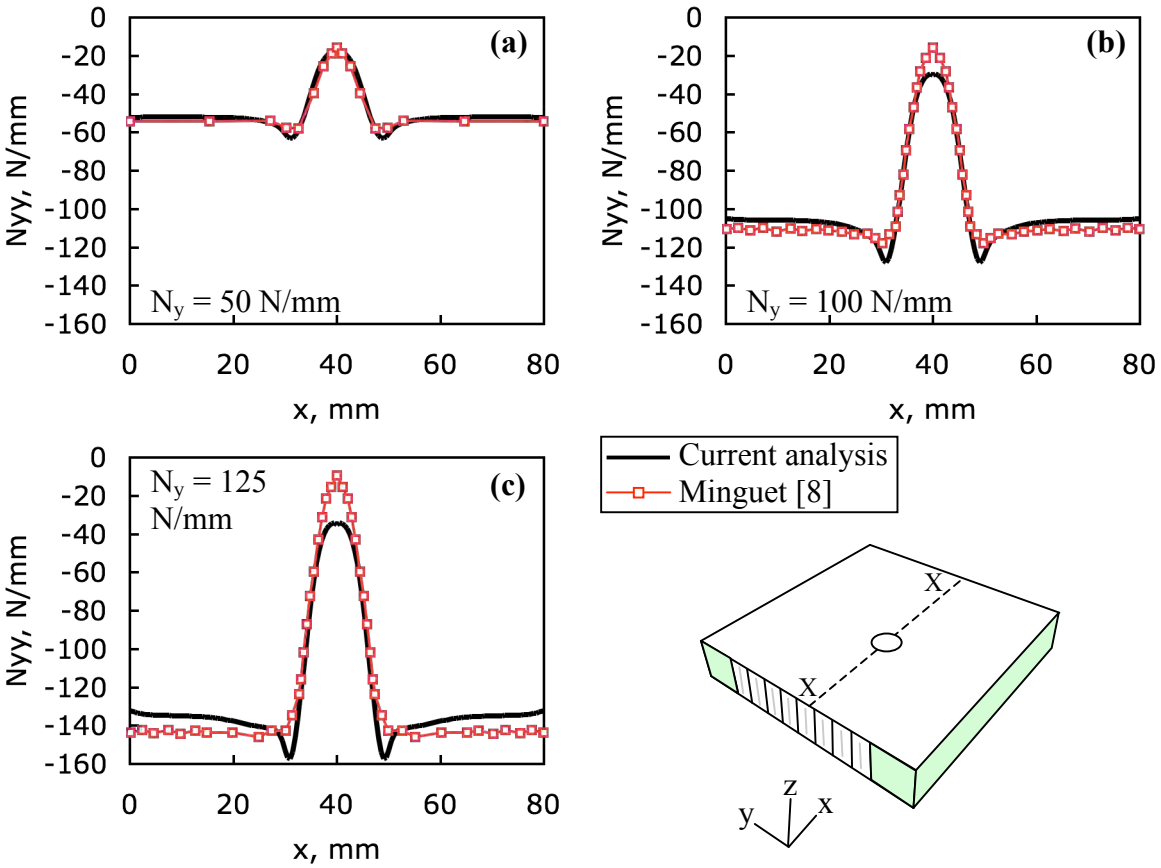

Figure 19. Distribution of in-plane reaction forces in facesheet along Line XX

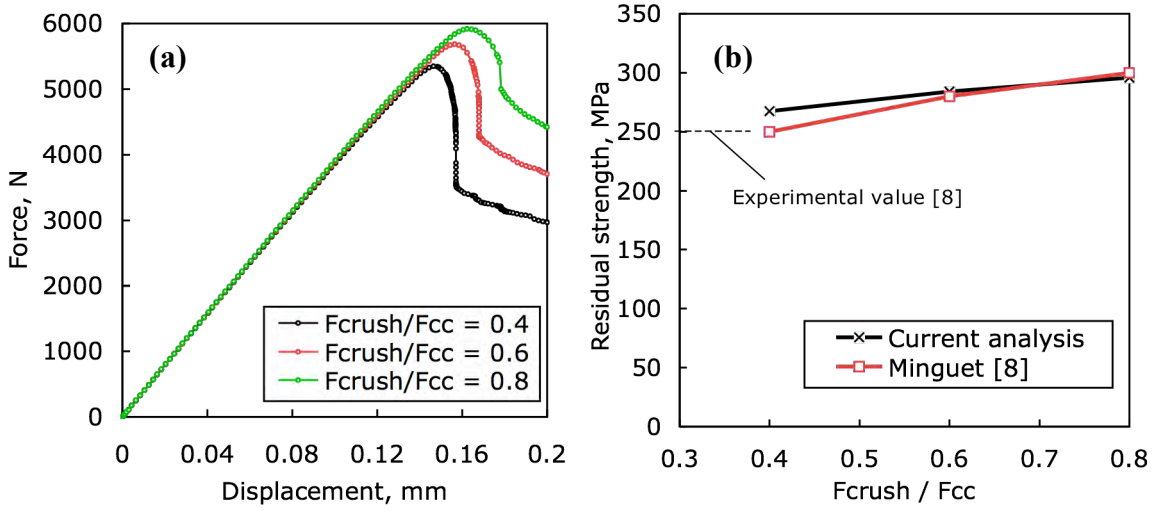

Figure 20. Effect of core crush ratio, F_{crush}/F_{cc} on force-displacement response and strength